RSC Advances

PAPER

View Article Online
View Journal | View Issue

Cite this: *RSC Adv.*, 2017, **7**, 52375

Facile fabrication of hybrid PA6-decorated TiO_2 fabrics with excellent photocatalytic, anti-bacterial, UV light-shielding, and super hydrophobic properties†

Shunli Zhou,[ab] Feng Wang,[*a] Subramanian Balachandran,[a] Gen Li,[a] Xiuqin Zhang,[*b] Rui Wang,[b] Peng Liu,[a] Yanfen Ding,[a] Shimin Zhang[a] and Mingshu Yang[a]

Self-cleaning fabrics decorated with titanium dioxide (TiO_2) nanoparticles (NPs) have garnered worldwide attention due to their outstanding ultraviolet (UV) light-shielding, anti-bacterial properties and other characteristics. Numerous techniques to construct super-antiwetting surfaces have been investigated for both fundamental research and practical application. A facile and eco-friendly way by a combination of UV irradiation and ultrasonic bath method has been developed to prepare a novel self-cleaning hybrid polyamine 6/nano TiO_2 (PA6/nano TiO_2) fabric with superhydrophobic and durable photocatalytic properties. To evaluate the fabric's reusability, hybrid PA6/nano TiO_2 fabrics were subjected to five consecutive cycles of the photocatalytic degradation of the methyl orange (MO) dye. The results indicated that TiO_2 NPs were firmly fixed on the fiber surface. The UV-blocking and anti-microbial properties of these hybrid fabrics were also tested. For PA6 immobilized by commercial nano TiO_2-P25 (P25-PA6) and PA6 immobilized by prepared visible-light photocatalyst PVA_D-TiO_2(PVA_D-PA6) fabrics, the UV protection factors (UPFs) of the samples were 56 and 1123, respectively. The anti-microbial efficacies of the two samples were both 99%. The water contact angles were 151.7° and 154.6°, respectively, indicating surface superhydrophobicity. These results showed that this novel fabric has great potential for indoor environmental purification and outdoor protection applications.

Received 30th August 2017
Accepted 6th November 2017

DOI: 10.1039/c7ra09613e

rsc.li/rsc-advances

1. Introduction

Polyamine 6 (PA6) fabric, a comfortable material with high abrasion resistance, has been widely used in many special cloth applications. PA is one of the most widely used fabrics in the textile industry due to its excellent mechanical properties, high thermal stability and chemical resistance. The outstanding wear resistance and low density of PA fabrics make it a superior choice for outdoor cloth. Hydrophobicity, ultraviolet (UV) resistance and anti-bacterial properties are essential for outdoor cloth because of the rugged environmental conditions.[1,2] However, until now it has remained a challenge to fabricate commercial PA outdoor cloths with those multi-functional properties.

The rapid development of nanotechnology provides opportunities for the innovation of novel nanomaterials.[3,4] Titanium dioxide (TiO_2) has been recognized as the most promising semiconductor catalyst in heterogeneous photocatalysis due to its large surface area, non-toxicity, low cost, chemical stability and many available facile fabrication methods.[5] TiO_2 can decompose a wide range of toxic organic species in air or water, mitigate organic pollutants, and kill microorganisms under UV light irradiation.[6–8]

Recently, substantial efforts have been expended to increase the mechanical stability of super hydrophobic fabrics. Super anti-wetting coatings on fabrics with high water contact angles show great prospect because of their exclusive water repulsion and self-cleaning properties.[9,10] The application of TiO_2 nanoparticles (NPs) in the fabrication of self-cleaning fabrics with excellent UV-blocking and anti-bacterial properties has attracted significant attention.[11–13] These innovative studies to prepare super hydrophobic, UV-blocking and anti-bacterial materials are promising, and further research is still needed for practical applications.

Considerable efforts have been devoted to the application of NPs on fabrics. Surface treatment of the fabric has been reported to be one of the most effective ways to enhance the interaction between NPs and fabrics.[7,14] Some researchers have embedded TiO_2 NPs in fabrics by chemical methods.[11,14–16] For

[a]*Beijing National Laboratory for Molecular Science, CAS Key Laboratory of Engineering Plastics, Institute of Chemistry, Chinese Academy of Sciences, Beijing 100190, P. R. of China. E-mail: wangfeng0822@iccas.ac.cn*

[b]*School of Materials Science & Engineering, Beijing Institute of Fashion Technology, Beijing, 100029, China. E-mail: clyzxq@bift.edu.cn*

† Electronic supplementary information (ESI) available. See DOI: 10.1039/c7ra09613e

example, Khajavi and co-workers explored the effect of the chain lengths of three dicarboxylic acids (oxalic, succinic, and adipic acids) on the self-cleaning properties and washing durability of cotton fabric.[16] They found that dicarboxylic acids increased the amounts of TiO_2 NPs absorbed onto cotton samples and improved their washing durability. Xu *et al.* immersed 3-chloro-2-hydroxypropyl trimethyl ammonium chloride (CHTAC) and 1,2,3,4-butanetetracarboxylic acid (BTCA)-modified cotton fabrics in TiO_2/SiO_2 hydrosol.[17] These authors found that the photocatalytic efficiencies and NP stabilities were improved, but the tensile strengths were decreased. Furthermore, the ionic crosslinking treatment increased the UV-blocking ability. However, the chemical method is environmentally unfriendly and potentially poisonous.[15]

Physical methods, such as plasma, UV irradiation,[18] corona[19] and ultrasonic bath,[20,21] are preferable because of their lower energy consumption, easier procedures, and higher efficiencies. These methods promote the formation of new active sites on the surface without deteriorating the inherent characteristics of the fabrics. Mejia and his co-workers employed UV-C (185 nm) and radio frequency (RF) plasma to pre-treat PA surfaces at atmospheric pressure and increased their interaction with TiO_2.[18] They found that both treatments increased the number of active sites on the surface of PA fabric. UV irradiation resulted in a good dispersion of the NPs, and pre-treatment increased photocatalytic decolouration of a red wine stain on PA-TiO_2, compared to the pristine fabric. Mohammad Mirjalili *et al.* used a corona method to pre-treat a cotton fabric with different intensities and irradiation times.[19] They found that the corona treatment improved the stabilization of the TiO_2 NPs on the cotton fabric surface, even after 50 washing cycles. Perelshtein used an ultrasonic bath to coat textiles with commercial NPs.[20,21] After ultrasonic bath treatment, the NPs were strongly anchored to the textile and the dispersion was more uniform. And the textile showed excellent anti-bacterial properties.

Many types of pollutants can be degraded by TiO_2 NPs under UV irradiation because of the outstanding photocatalytic performance. However, the wide band gap is 3.2 eV, and thus, only UV light can activate the TiO_2 NPs. Substantial research has been dedicated to the utilization of solar energy,[22–24] such as surface modification of NPs and doping with other elements. In our previous work, we prepared conjugation-grafted-TiO_2 hybrid NPs to achieve high photocatalytic efficiency under visible light by modifying Degussa P25 with partially degraded polyvinyl alcohol (PVA).[25]

In this work, we described an efficient way to synthesize PA6/nano TiO_2 fabric. UV irradiation was applied to modify the surface of the PA6 fabric, and an ultrasonic bath was used to disperse the NPs uniformly on the fabric. The structures of the resulting hybrid PA6/nano TiO_2 fabrics were characterized. The photocatalytic efficiency, UV-blocking ability, anti-bacterial properties, and super hydrophobicity of the hybrid fabrics were also investigated. The results showed that this novel fabric has great potential for indoor environmental purification and outdoor protection applications.

2. Experimental section

2.1 Materials

Pure PA6 fabric was purchased from Guangdong Xinhui Meida PA Co. Ltd (China). Methyl orange (MO, $(H_3C)_2NC_6H_4N_2C_6H_4$-SO_3Na) was obtained from Beijing Chemical Works (China). Span 80 was purchased from Sinopharm Chemical Reagent Co. Ltd. $NaHCO_3$ was acquired from Beijing Chemical Works. PVA and PEG were purchased from Yili Chemical Works (China). TiO_2-P25 (80% anatase and 20% rutile with a Brunauer–Emmett–Teller (BET) surface area of 50 $m^2\ g^{-1}$ and a mean particle size of 30 nm) was supplied by Evonik (Germany). Deionized water was employed in all experiments.

2.2 Sample preparation

Preparation of PVA_D-*g*-TiO_2 and TiO_2 hydrosol. PVA-modified Degussa P25 TiO_2 (PVA_D-*g*-TiO_2) was prepared according to our previous work.[25] One gram of P25 TiO_2 NPs and 1 g of PVA_D-*g*-TiO_2 were dispersed in deionized water, stirred for 4 h, and then immersed in ultrasonic bath for an additional 2 h.

Surface treatment of PA6 fabrics. Prior to the coating process, PA6 fabric was immersed in a solution containing 1 g L^{-1} Span 80, a non-ionic detergent, and 5 g L^{-1} $NaHCO_3$ at 60 °C and stirred for 1 h to remove surface impurities. The fabric was then rinsed with deionized water, dried at room temperature for 24 h, and cut into 3 × 10 cm samples. The samples were put into a UV Crosslinker (light source = 254 nm, UVP CL-100, USA) for the designated time. The fabrics were immediately immersed into the hydrosol, placed into the ultrasonic bath for 30 min, and dried in an oven at 60 °C for 10 min. Then, fabrics were again immersed into the hydrosol and ultrasonic bath for an additional 30 min and placed in the oven for 10 min. The samples were subsequently heated in a vacuum oven at 140 °C and −0.1 atm for 2 h. The samples are labelled as P25-PA6 and PVA_D-PA6.

2.3 Characterization

To characterize the surface morphology, platinum-coated fabric samples were examined using a scanning electron microscopy (SEM, JOEL-6700, Japan). NPs losses were evaluated by thermal gravity analysis (Pyris 1, Perkin Elmer, US), the samples were heated from 100 °C to 750 °C in 5 °C min^{-1} under air atmosphere to remove the PA6 fabrics. The surface topology was evaluated using an atomic force microscopy (AFM, Bruker Multimode 8, Germany). To analyze the samples' UV-block property, UV absorbance measurements were collected using a SHIMADZU UV-2600 spectrometer (UV-vis, SHIMADZU, Japan). A drop shape analyzer (DSA-100, Kruss, Germany) was applied to determine the water contact angle. X-ray photoelectron spectra (XPS, VG Scientific, ESCALab220i-XL) was used to study the elements distribution on the surface of the samples. The stability of the surface functional groups was examed by FTIR/ATR (Thermo Nicolet 6700 FTIR). X-ray diffraction (XRD,

Japan, Rigaku D/max-2500) was employed to characterize the crystal type of the samples.

Photocatalytic degradation tests. Photocatalytic degradation tests were conducted under UV and visible light irradiation. To evaluate the photocatalytic efficiency, MO was dissolved in an aqueous solution at an initial concentration of 15 mg L^{-1}, and the samples were immersed in 30 mL of MO solution. UV light degradation was conducted in a UVP CL-100 instrument, and the visible light degradation test was performed in the photochemical reactor used in our previous work. Prior to degradation, the samples were equilibrated in the dark for 2 h to eliminate the effect of adsorption. Degradation experiments were conducted over a designated time period, and 3 mL aliquots of the solution were withdrawn at specified time intervals for concentration analysis using a Hitachi-U-2001 spectrometer (UV, Hitachi, Japan); the aliquots were later returned to the reaction vessel to continue the test.

Wash fastness. The stability of Nano TiO_2 particles on the fabric was evaluated by a simulated laundry test. The procedure of laundry test is as following. At first, the samples were added to a big beaker which is full of cloth, water and some detergent. Then the cloth was stirred with a speed of 500 rpm for 50 h, finally the loss of NP loss was calculated by TGA tests.

Anti-bacterial activity. The anti-bacterial activities of the PA6/nano TiO_2 fabrics under visible light were determined by an authorized testing faculty using the GB/T 30707-2014 measurement method. *Staphylococcus aureus* (ATCC 6538), Gram-positive bacteria which had been incubated in nutrient agar at 37 °C for 24 h, was selected as the representative test organism. An inoculating loop was used to transport the bacteria to a nutrient broth (NB) solution, and then, tenfold dilution were performed until a test solution containing 5–20 × 10^5 colony-forming units (CFU mL^{-1}) was acquired. Six pieces of each sample fabric were placed in six Petri dishes, and the bacterial suspension was dripped onto each test piece. Inert and non-water-absorbent polyethylene (PE) films with good sealing properties and an optical transmittance exceeding 85% for the 380–780 nm range were used as cover films. The cover films were placed on the suspensions, and moisture conservation glasses were placed on top of the Petri dishes. Three Petri dishes containing test pieces were exposed to light, and the other three were kept in the dark. Nine pieces of blank fabric were tested: three as post-inoculation specimens, three as blanks exposed to light with the test pieces, and three kept in the dark. After the test, the test bacteria were washed off from each test piece and cover film. Post-inoculation specimens were washed immediately after inoculation, and the initial number of bacterial colonies was counted. This washout suspension was measured by the viable bacterial count method. The test pieces were cut into 50 mm × 50 mm samples, and plain glass was used as blank samples. The test was conducted under visible light sources with UV light filtered out and a light intensity of 2500 Lx, and each experiment lasted 24 h. UV light was utilized to disinfect the samples 12 h before the test. To ensure uniform illumination, the samples were rotated after 12 h. The results are presented as the average number of CFU based on the analysis of three pieces of fabric.

The anti-bacterial rate R_{total} was calculated with the following formula:

$$R_{total} = (C_0 - C_1)/C_0 \times 100$$

C_0: the average number of viable bacteria on blank samples after indoor light illumination. C_1: the average number of viable bacteria on samples after indoor light illumination.

The indoor light-active photocatalytic anti-bacterial activity after indoor light illumination R_{light} was calculated using the following formula:

$$R_{light} = (B_1 - C_1)/B_1 \times 100$$

B_1: the average number of viable bacteria on samples after being kept in the dark.

Water contact angle measurements. The wettability of the samples was evaluated by contact angle analysis (Kruss DSA100). A drop of water (4 μL) was deposited on pristine PA6 or TiO_2-impregnated samples, and the angle was estimated using software to fit the photograph taken by the instrument. Measurements were repeated at least three times for each sample.

3. Results and discussion

3.1 Characterization of PA6/nano TiO_2 fabrics

Field Emission SEM (FESEM) were performed to study the morphology of pristine PA6 fabric and PA6 fabric irradiated

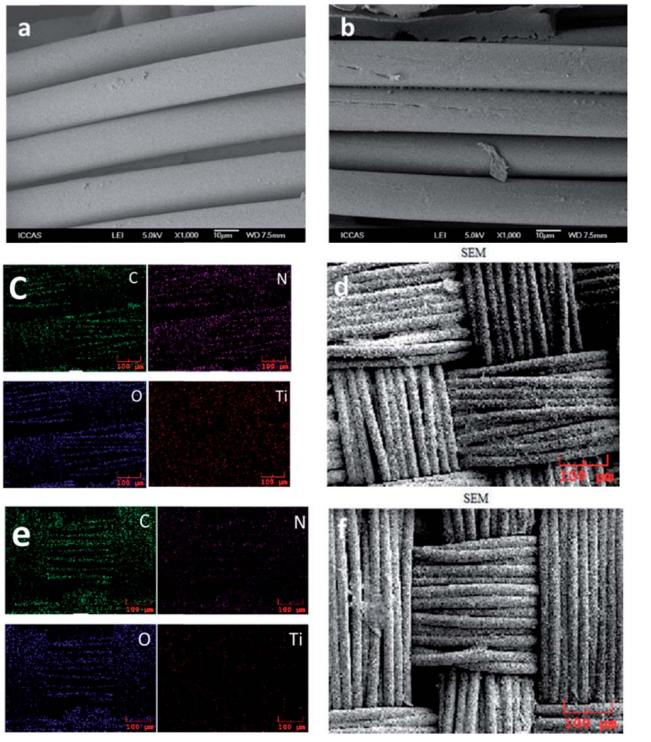

Fig. 1 (a) Pristine PA6 fabric and (b) PA6 fabric irradiated with UV light for 30 min. C, O, N, and Ti elemental color mapping results of P25-PA6 (c) and PVA_D-PA6 (e). FESEM images of P25-PA6 (d) and PVA_D-PA6 (f).

under UV light, which were showed in Fig. 1a and b, respectively. After 30 min of UV irradiated, the PA6 had developed a rough surface, compared with the smooth surface of the pristine PA6 fabric. Cavities were observed on the surface, indicating that UV irradiation caused physical and/or chemical modification of the PA6 fibres (Fig. 1a and b). According to Mejia,[18] UVC activation with lower energy than RF plasma, could generate atomic and excited oxygen species, whereas UVA irradiation resulted in a more uniform distribution of TiO_2 NPs.

Elemental mapping was carried out by using FE-SEM to identify the components of hetero-architectured P25-PA6 and PVA_D-PA6. Fig. 1 showed the elemental mapping results for these elements and a survey spectrum of the FESEM images. Clearly, the densities of C, O and N are higher than that of Ti; Ti exhibits a homogenous distribution; and the catalyst is composed of C, O and Ti. These results also confirmed the purity of the P25-PA6 and PVA_D-PA6 fabrics. Interestingly, the density of Ti signals of the P25-PA6 sample is higher than that of the PVA_D-PA6 sample because the TiO_2 NPs were wrapped by carbon-based conjugated structures embedded in the PVA_D-PA6.[25]

To identify the element valence states in P25-PA6 and PVA_D-PA6 fabrics, X-ray photoelectron spectroscopy (XPS) was performed. Based on previously reported XPS analyses,[26–28] the peak with the binding energy (BE) of 284.7 eV in Fig. 2b is attributed to carbon atoms from PA6 molecules. The peak at 285.2 eV was assigned to carbon atoms bound to the carbonyl groups in PA6, and the peak at 286.4 eV was attributed to carbon atoms bonded to the –NH– group in PA6. The peak at 289.0 eV in Fig. 2e corresponded to carbonyl carbons in TiO_2. In the O 1s spectrum, the main peak at 532.3 eV corresponded to the carbonyl oxygens in PA6 molecules, whereas the shoulder peak at 529.9 eV attributed to the oxygen atoms of TiO_2. The Ti 2p1/2 and Ti 2p3/2 spin–orbital splitting photoelectrons detected in both samples have BEs of 464.48 and 458.72 eV, respectively, as seen in Fig. 2. The peak separation (5.86 eV) between the Ti 2p1/2 and Ti 2p3/2 signals is in excellent agreement with the literature.[29]

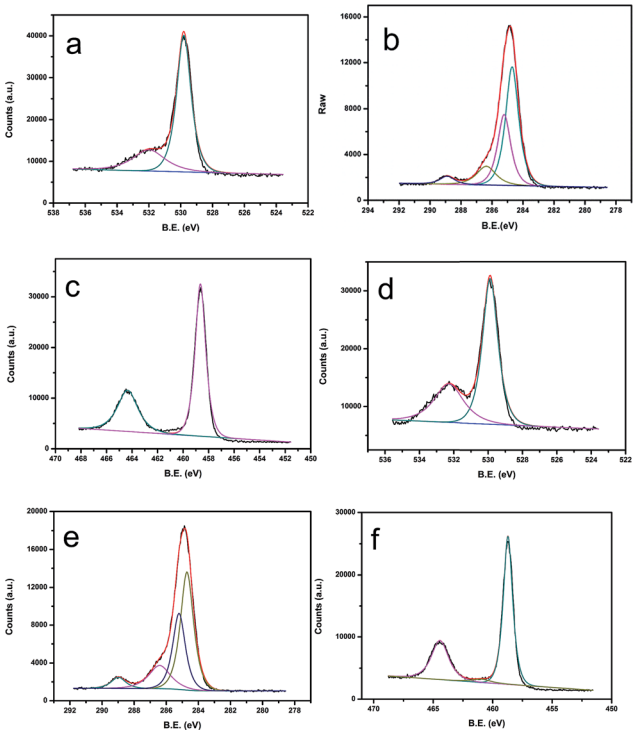

Fig. 2 (a) O 1s, (b) C 1s, and (c) Ti 2p XPS spectra of the P25-PA6 sample. (d) O 1s, (e) C 1s, and (f) Ti 2p XPS spectra of the PVA_D-PA6 sample.

3.2 Photocatalytic degradation under visible light

To explore photocatalytic degradation under visible light, pure MO and a PA6-MO blank were used as controls. Prior to the visible light degradation experiments, the samples were placed in the dark to reach adsorption–desorption equilibrium. The results presented in Fig. 3 show that the pure MO curve changed slightly, indicating that the pure MO solution was not degraded under visible light. In contrast, the concentration of the pure PA6-MO solution decreased by nearly 15% at the end of the experiment which was attributed to the absorption of the PA6 fabric. No photocatalytic effect was observed by using the pure PA6 sample, and after 2 h exposure in the dark, the absorption did not reach equilibrium. Commercial Degussa P25 NPs are known to exhibit poor performance for visible light photocatalytic degradation because of their wide band gap, as observed in the P25-PA6 curve. Compared to P25-PA6, the PVA_D-PA6 sample exhibited excellent visible light photocatalytic efficiency. Indeed, the visible light photocatalytic degradation rate constant of PVA_D-PA6 was calculated to be 0.113, whereas P25-PA6 was 0.049. The degradation rate constant of PVA_D-PA6 was 2.3 times higher than that of P25-PA6 sample after correcting for the absorption factor. Our previous work demonstrated that PVA_D-*g*-TiO_2 NPs have excellent photocatalytic properties under visible light irradiation because of the effective visible light harvest by the conjugated structures of the degraded polymer layer and efficient electron transfer through the C–O–T bonds between TiO_2 and conjugated structures.

3.3 Successive cycles of photocatalytic degradation

Five successive cycles of photocatalytic degradation were conducted to test the durability of the fabrics (Fig. 4). This experiment was conducted under UV light, and at the end of each cycle, the samples were taken out, washed with deionized water,

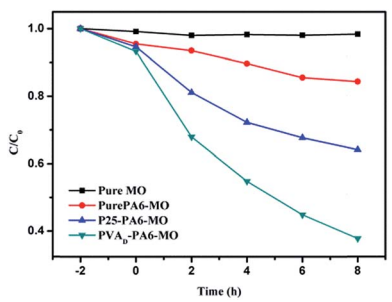

Fig. 3 Photocatalytic degradation curves under visible light irradiation.

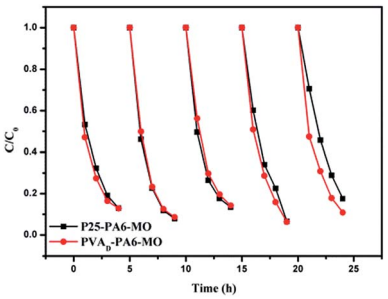

Fig. 4 Five successive cycles of photocatalytic degradation under UV light using P25-PA6 and PVA_D-PA6.

and dried in an oven at 60 °C before the next photocatalytic degradation cycle. The results clearly showed that under UV light, the P25-PA6 sample's photocatalytic efficiency was similar to that of PVA_D-PA6. After five photocatalytic degradation cycles, little difference was observed in the photocatalytic efficiencies of both samples. It was concluded that the samples were durable and strong interactions exist between PA6 fabrics and TiO_2 NPs.

To measure the NP loss after five degradation cycles, thermogravimetric analysis (TGA) was conducted. To measure the NPs left, the initial NP weight percent of P25-PA6 was 6.086%, which decreased to 5.981% after five cycles. The initial weight percent of the PVA_D-PA6 was 6.872%, which decreased to 5.964% after five cycles. The weight loss of both samples was limited, in agreement with the photocatalytic efficiency results.

According to Agnes Rages, UV irradiation at atmospheric pressure may cause the conversion of O_2 to the extremely active $O^{\bullet}$ radical, resulting in active groups, such as –OH and –NH, on the surface of the fabric.[30] These groups could react with the –OH on the surface of TiO_2 NPs, and enhanced the interactions between the NPs and the fabrics.

The TGA curves of the samples after laundry tests were presented in Fig. 5. The results showed that primary P25 weight is 6.81%, after 50 h luandry test, the P25 weight decreased slightly to 6.25%. And the PVAD-PA6 sample decreased from 11.91% to 9.59%, which proved that both the samples have good fastness.

3.4 Antimicrobial properties

The antimicrobial rate of P25-PA6 and PVA_D-PA6 samples have been improved significantly compared with the pure PA6 fabric and the anti-bacterial rate of P25-PA6 sample was nearly the same as that of the PVA_D-PA6 sample. In Table 1, we can see that the P25-PA6 samples have low CFU compared to the PVA_D-PA6 sample in the darkness, indicating that the P25-PA6 sample has increased bacterial resistance compared with the PVA_D-PA6 sample.

The R_{light} of the P25-PA6 sample was 91%, whereas that of PVA_D-PA6 was 94%, demonstrating that the PVA_D-PA6 sample had a superior anti-bacterial effect than P25-PA6 with greater potential for application as an indoor light-active photocatalytic anti-bacterial material. In general, the P25-PA6 sample exhibited better anti-bacterial properties in the dark, whereas the PVA_D-PA6 sample exerted a better indoor light-active photocatalytic anti-bacterial effect.

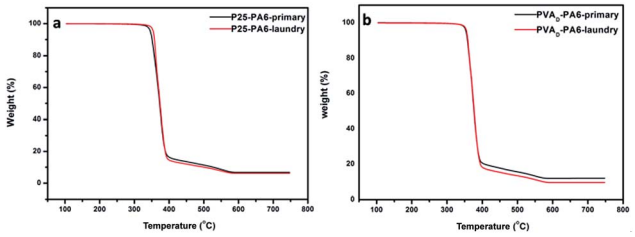

Fig. 5 The TGA curves of the (a) P25-PA6 and (b) PVA_D-PA6 before and after laundry test.

3.5 UV-shielding property

UV-shielding property is important for outdoor cloth. To study the UV-blocking properties, the UV protection factors (UPFs) of the samples were determined according to the GB/T 18830-2002 method. These tests were conducted by a UV light source with a wavelength in the range of 290–400 nm using an integrating sphere to collect all the transmitted light. Each sample was placed in front of the integrating sphere, and its transmittance was monitored in the range of 290–400 nm by recording values at 5 nm intervals. The UPF was calculated as follows:[31]

$$\mathrm{UPF} = \frac{\int_{290}^{400} E_\lambda S_\lambda \mathrm{d}\lambda}{\int_{290}^{400} E_\lambda S_\lambda T_\lambda \mathrm{d}\lambda}$$

where λ is the wavelength (nm), $E(\lambda)$ is the relative erythermal effectiveness, $\varepsilon(\lambda)$ is the solar UV spectral irradiance (W m^{-2} nm^{-1}), $T(\lambda)$ is the spectral transmittance of the fabric, and $\Delta(\lambda)$ is the wavelength increment (nm). UPF values of 15–24 correspond to good protection against UV light, values of 25–39 to very good protection against UV light, and values of 40–50+to excellent protection against UV light.

The curves in Fig. 6 showed that the UV transmittance of the pristine PA6 fabric was much higher than those of the P25-PA6 and PVA_D-PA6 samples. Using the above formula, the UPF of pure PA6 was calculated to be 3. For the P25-PA6 and PVA_D-PA6 samples, the UV light transmittance in the range of 290–370 nm reached zero, indicating that UVB light was completely blocked. Additionally, the PVA_D-PA6 sample exhibited better UV light shielding in the range of 370–400 nm than the P25-PA6 sample, which could be attributed to the excellent visible light absorbance of PVA_D-*g*-TiO_2. The UPF of P25-PA6 was 56, whereas PVA_D-PA6 was 1233. This astounding value was ascribed to its the excellent light shielding in the range of 370–400 nm relative to that of the P25-PA6 sample.

3.6 Water contact angle

Water contact angle and AFM images were presented in Fig. 7. Pure PA6 fabric was a hydrophilic material, and the contact angle was 33°. The contact angle of the P25-PA6 sample was measured to be 151.7°, and PVA_D-PA6 sample was 154.6°. Therefore, both samples became super hydrophobic from

Table 1 Anti-bacterial properties of the samples

	Staphylococcus aureus ATCC 6538				
	Average of the viable cell (CFU per piece)			Anti-microbial rate R_{total} (%)	Value of anti-microbial activity R_{light} (%)
	0 h	24 h (dark)	24 h (light)		
Blank	1.3×10^4	4.5×10^5	2.2×10^5	—	—
Pure PA6	—	8.0×10^5	7.7×10^4	65	90
P25-PA6	—	2.7×10^4	2.4×10^3	99	91
PVA_D-PA6	—	4.6×10^4	2.9×10^3	99	94

hydrophilic after the TiO_2 NPs were embedded on their surfaces. The results of water contact angle hysteresis were as follows: pure PA6 is 25°, P25-PA6 is 16°, and PVAD-PA6 is 18°. The surface morphology also changed significantly as observed in the SEM and AFM images. The surface of the pristine PA6 was smooth, and the AFM images indicated that the surface altitude varied by several nanometres. In contrast, the surfaces of P25-PA6 and PVA_D-PA6 samples were covered by micro-sized bulges composed of TiO_2 NP structures, which affected their water contact angles.[32] The surface altitudes of the P25-PA6 and PVA_D-PA6 samples varied by approximately 100–200 nm, confirmed by the AFM image. According to Jiang's work,[33,34] the key factors leading to super hydrophobicity include the surface energy of the chemical composition and a geometrically rough structure of the solid surface. The SEM images also revealed the formation of lotus-like surface structures on the two samples. This phenomenon may also support the achievement of good distributions of NPs on the fabric surface by an ultrasonic bath.

To evaluate the stability of the surface structure under acidic and basic conditions, the samples were separately immersed in the hydrochloric acid solution (pH = 1) and sodium hydroxide solution (pH = 14) for 2 h. Then the samples rinsed in deionized water, and were dried in the oven to test the water contact angle. To evaluate the stability of the surface structure against frictional force, the water contact angle of the samples which after simulated laundry were tested. The water contact angle images could be seen in Fig. S6.†

The water contact angle of (a) P25-PA6 after acidic condition was 152.9°, and (b) P25-PA6 after basic condition was 147.4°. And the water contact angle of (c) PVA_D-PA6 after acidic conditions was 153.6° and (d) PVA_D-PA6 after basic condition was 154.3°. The results showed that the surface structure of the samples all kept steady after harsh conditions. The water contact angle of (e) P25-PA6 after simulated laundry decreased to 123.2° and (f) PVA_D-PA6 after simulated laundry 97.1°. It could be concluded that the stability of the surface structure against acidic condition and basic condition is excellent, but the stability against frictional force should be improved.

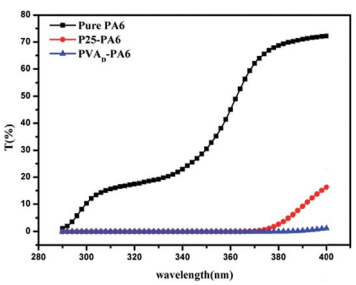

Fig. 6 UV light transmittance curves of the three samples.

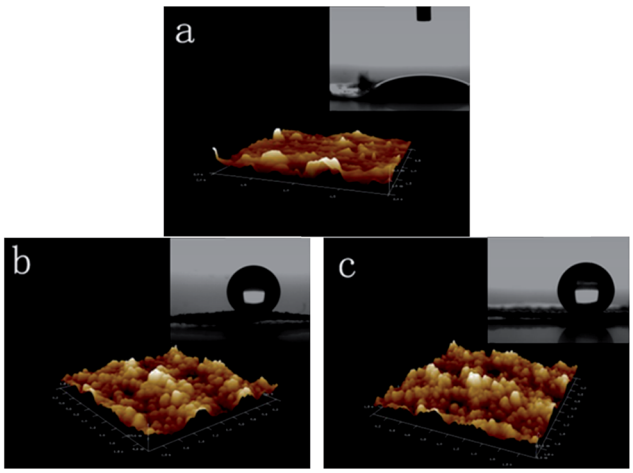

Fig. 7 Water contact angle determination and AFM images of (a) pristine PA6 fabric, (b) the P25-PA6 sample, and (c) the PVA_D-PA6 sample.

4. Conclusion

In summary, we developed a green method to embed two types of TiO_2 NPs in PA6 fabrics *via* UV irradiation and ultrasonic bath treatment. The results showed that 30 min of UV irradiation resulted in the best photocatalytic efficiency and high durability. The PVA_D-PA6 fabric exhibited excellent photocatalytic efficiency under visible light irradiation. In addition, both samples displayed attractive anti-bacterial and UV-shielding properties. The water contact angle results demonstrated that both samples were super hydrophobic. These hybrid PA6/nano TiO_2 fabrics have great potential for applications in toxic dye removal and in anti-bacterial, UV light-shielding and super hydrophobic materials.

Conflicts of interest

There are no conflicts to declare.

Acknowledgements

This study was financially supported by the National Natural Science Foundation of China (Grant No. 51403217 and 51534007), New Century Excellent Talents in University (Contract grant number NCET-12-0601), the Youth Innovation Promotion Association of CAS (Grant No. 2017041) and the "Strategic Priority Research Program" of the Chinese Academy of Sciences (Grant No. XDA09030200).

Notes and references

1 V. V. Vinogradov, A. V. Agafonov and A. V. Vinogradov, *Mendeleev Commun.*, 2013, **23**(5), 286–288.
2 A. E. Tayyar and G. Alan, *J. Text. Inst.*, 2014, **106**(3), 303–310.
3 V. Singh, D. Joung, L. Zhai, S. Das, S. I. Khondaker and S. Seal, *Prog. Mater. Sci.*, 2011, **56**(8), 1178–1271.
4 J. Bogdan, A. Jackowska-Tracz, J. Zarzynska, *et al.*, *Nanoscale Res. Lett.*, 2015, **10**, 57.
5 C. W. Kim, U. Pal, S. Park, Y. H. Kim, J. Kim and Y. S. Kang, *RSC Adv.*, 2012, **2**, 11969.
6 J. Mo, Y. Zhang, Q. Xu, J. J. Lamson and R. Zhao, *Atmos. Environ.*, 2009, **43**(14), 2229–2246.
7 M. Radetić, *J. Photochem. Photobiol., C*, 2013, **16**, 62–76.
8 M. Pal, U. Pal, R. Silva Gonzalez, E. Sanchez Mora and P. Santiago, *J. Nano Res.*, 2009, **5**, 193–200.
9 M. Montazer and E. Pakdel, *J. Photochem. Photobiol., C*, 2011, **12**(4), 293–303.
10 W. Shen, C. Zhang, Q. Li, W. Zhang, L. Cao and J. Ye, *J. Cleaner Prod.*, 2015, **87**, 762–765.
11 A. Nazari, M. Montazer, A. Rashidi, M. Yazdanshenas and M. Anary-Abbasinejad, *Appl. Catal., A*, 2009, **371**(1–2), 10–16.
12 E. Pakdel, W. A. Daoud and X. Wang, *Appl. Surf. Sci.*, 2013, **275**, 397–402.
13 X. Jiang, X. Tian, J. Gu, D. Huang and Y. Yang, *Appl. Surf. Sci.*, 2011, **257**(20), 8451–8456.
14 A. Nazari, M. Montazer and M. B. Moghadam, *Carbohydr. Polym.*, 2011, **83**(3), 1119–1127.
15 A. Farouk, S. Sharaf and M. M. Abd El-Hady, *Int. J. Biol. Macromol.*, 2013, **61**, 230–237.
16 R. Khajavi and A. Berendjchi, *ACS Appl. Mater. Interfaces*, 2014, **6**(21), 18795–18799.
17 Z. J. Xu, Y. L. Tian, H. L. Liu and Z. Q. Du, *Appl. Surf. Sci.*, 2015, **324**, 68–75.
18 M. I. Mejia, J. M. Marin, G. Restrepo, C. Pulgarin, E. Mielczarski, J. Mielczarski, I. Stolitchnov and J. Kiwi, *ACS Appl. Mater. Interfaces*, 2009, **1**(10), 2190–2198.
19 M. Mirjalili, L. Karimi and A. Barari-tari, *J. Text. Inst.*, 2014, **106**(6), 621–628.
20 P. Petkova, A. Francesko, M. M. Fernandes, E. Mendoza, I. Perelshtein, A. Gedanken and T. Tzanov, *ACS Appl. Mater. Interfaces*, 2014, **6**(2), 1164–1172.
21 I. Perelshtein, G. Applerot, N. Perkas, J. Grinblat, E. Hulla, E. Wehrschuetz-Sigl, A. Hasmann, G. Guebitz and A. Gedanken, *ACS Appl. Mater. Interfaces*, 2010, **2**(7), 1999–2004.
22 L. Karimi, S. Zohoori and A. Amini, *New Carbon Mater.*, 2014, **29**(5), 380–385.
23 L. Karimi, M. E. Yazdanshenas, R. Khajavi, A. Rashidi and M. Mirjalili, *Cellulose*, 2014, **21**(5), 3813–3827.
24 R. Rahal, T. Pigot, D. Foix and S. Lacombe, *Appl. Catal., B*, 2011, **104**(3–4), 361–372.
25 P. Lei, F. Wang, S. Zhang, Y. Ding, J. Zhao and M. Yang, *ACS Appl. Mater. Interfaces*, 2014, **6**(4), 2370–2376.
26 F. S. Ohuchi and S. C. Freilich, *J. Vac. Sci. Technol., A*, 1986, **4**(3), 1039–1045.
27 A. P. Pijpers and R. J. Meier, *J. Electron Spectrosc. Relat. Phenom.*, 1987, **43**(2), 131–137.
28 J. L. Jordan, P. N. Sanda, J. F. Morar, C. A. Kovac, F. J. Himpsel and R. A. Pollak, *J. Vac. Sci. Technol., A*, 1986, **4**(3), 1046–1048.
29 E. McCafferty and J. P. Wightman, *Surf. Interface Anal.*, 1998, **26**(8), 549–564.
30 R. Agnes, S. Danial and L. Jacques, *Macromolecules*, 1985, **18**, 1771–1775.
31 C. Welsh and B. Diffey, *Clin. Exp. Dermatol.*, 1981, **6**, 577–582.
32 Y. Li, J. Wang, Y. Kong, J. Zhou, J. Wu, G. Wang, H. Bi, X. Wu, W. Qin and Q. Li, *Sci. Rep.*, 2016, **6**, 19187, DOI: 10.1038/srep19187.
33 X. Shi, R. Dou, T. Ma, W. Liu, X. Lu, K. J. Shea, Y. Song and L. Jiang, *ACS Appl. Mater. Interfaces*, 2015, **7**(33), 18424–18428.
34 X. J. Feng and L. Jiang, *Adv. Mater.*, 2006, **18**(23), 3063–3078.